nature communications

Article

https://doi.org/10.1038/s41467-023-40978-4

Cobalt-catalyzed atroposelective C–H activation/annulation to access N–N axially chiral frameworks

Received: 8 May 2023

Accepted: 17 August 2023

Published online: 29 August 2023

Check for updates

Tong Li[1,2], Linlin Shi[1,2], Xinhai Wang[1], Chen Yang[1], Dandan Yang[1] ✉, Mao-Ping Song[1] & Jun-Long Niu[1] ✉

The N–N atropisomer, as an important and intriguing chiral system, was widely present in natural products, pharmaceutical lead compounds, and advanced material skeletons. The anisotropic structural characteristics caused by its special axial rotation have always been one of the challenges that chemists strive to overcome. Herein, we report an efficient method for the enantioselective synthesis of N–N axially chiral frameworks via a cobalt-catalyzed atroposelective C-H activation/annulation process. The reaction proceeds under mild conditions by using $Co(OAc)_2{\cdot}4H_2O$ as the catalyst with a chiral salicyloxazoline (Salox) ligand and O_2 as an oxidant, affording a variety of N–N axially chiral products with high yields and enantioselectivities. This protocol provides an efficient approach for the facile construction of N–N atropisomers and further expands the range of of N–N axially chiral derivatives. Additionally, under the conditions of electrocatalysis, the desired N–N axially chiral products were also successfully achieved with good to excellent efficiencies and enantioselectivities.

Atropisomerism, as one kind of intriguing axial chirality, has greatly aroused explosive attention due to their fascinating architectures and excellent multidisciplinary applications (pharmaceutical exploitation, functional materials development), arising from the restricted rotation around a single bond[1–5]. Since the pioneering work by Kenner on the expound of axial chirality from the perspective of fabrication and development significance via organic synthetic tactics in early 19th century[6], innumerable atropisomerism-based skeletons have been continually discovered due to the continuous progress in preparation, separation, purification methods and instruments. In this context, C–C and C–N atropisomers, including axially chiral biaryls, aryl amines, and aryl amides, are emerging at an amazing speed, and a variety of innovative achievements have been sparkled over the past two decades[7–19]. The atropisomerism of N–N bond, however, eluded such serious attention for a long time, which might be attributed to the incorrect notion that N–N axis is unstable due to the deplanarization effect. Indeed, the electronic barrier stemming from the repulsive interaction between the lone pairs on the two nitrogen atoms can strongly favor the formation of such atropisomers. These intriguing atropisomerism configurations have moved onto the research stage again due to the new structural understanding, making them a superior platform for serving N–N axial natural products, bioactive molecules, functional materials, and ligands production (Fig. 1a)[20–25]. By contrast, the atropisomerism bearing a N–N bond remains largely underdeveloped, possibly due to the shorter length and weaker nature of the N–N bond[26]. Besides, the low rotational barrier caused by the two *N*-containing planes deplanarization, renders the N–N axis construction more challenging. Typically, the N–N axially chiral skeletons could be built up through four types of transformations (Fig. 1b). The atroposelective N–H functionalization, such as allylation, alkylation, and acylation, represents an effective mean by modifying the central N–N axis[27–30]. Alternatively, catalytic asymmetric desymmetrization of pro-chiral substrates[31,32], and asymmetric assembly via de novo construction of pyrroles and indoles[33–37] also provide satisfactory choices

[1]College of Chemistry, Zhengzhou University, Zhengzhou 450001, P. R. China. [2]These authors contributed equally: Tong Li, Linlin Shi.
✉e-mail: yangdandan@zzu.edu.cn; niujunlong@zzu.edu.cn

https://doi.org/10.1038/s41467-023-40978-4

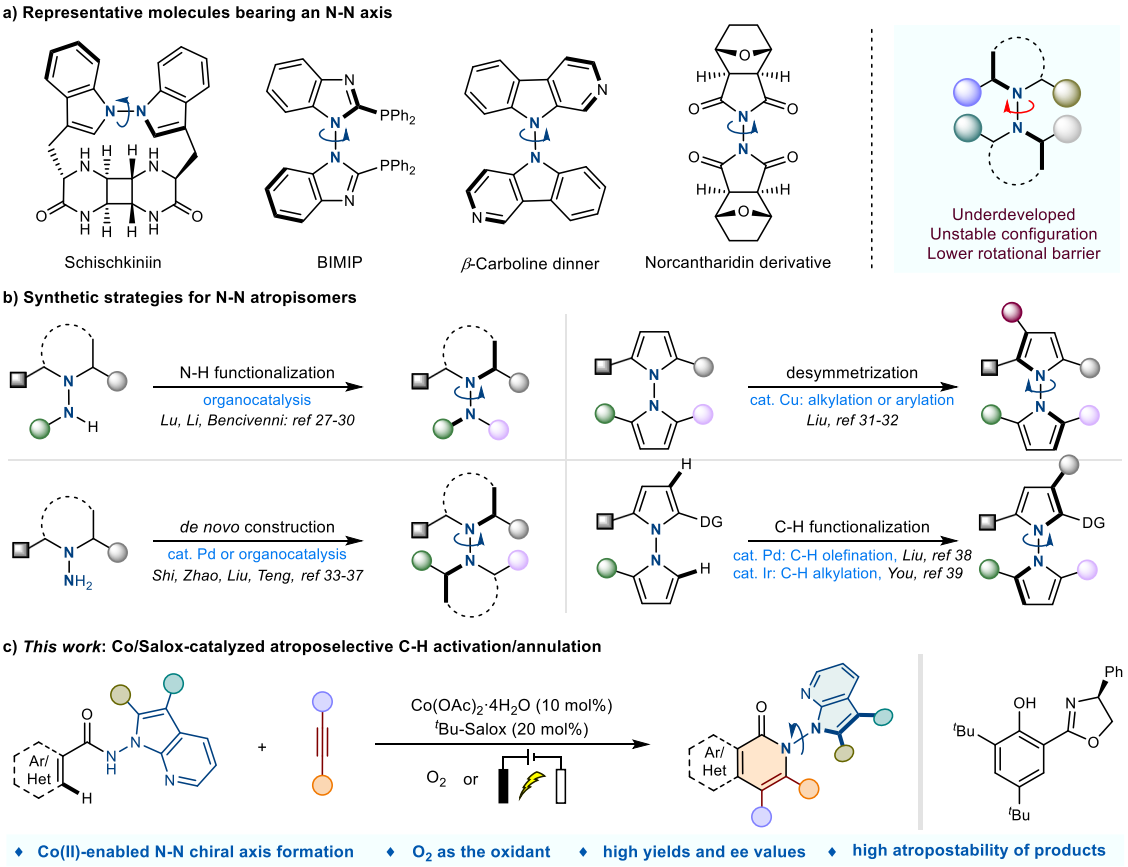

Fig. 1 | Background and project synopsis. a Representative molecules bearing an N–N axis. **b** Synthetic strategies for N–N atropisomers. **c** This work: Co/Salox-catalyzed atroposelective C–H activation/annulation.

for creating N–N atropisomers. Typically, Shi group have recently achieved organocatalytic enantioselective construction of N–N axially chiral indoles and pyrroles[36,37]. More recently, Liu and You groups successfully reported the construction of N–N atropisomers via the Pd or Ir-catalyzed C–H functionalization of indole/pyrrole ring through dynamic kinetic resolution of racemic N–N biaryls[38,39], further advancing the development of this field. Despite the elegant efforts made, research in this area is still in its infancy and remains underdeveloped. As a result, the development of more efficient and facile approaches for building novel and diverse N–N atroposelective frameworks is highly appealing yet challenging.

For this purpose, asymmetric C–H functionalization, as a timely emerged and well-established tactic, was built up to form diverse charming structures containing highly functionalized skeletons, such as natural products, pharmaceutical lead compounds, important architectures which typically takes advantage of batch production with satisfactory chemical selectivity (stereoelectronic selectivity and regioselectivity) via transition metal catalyzed process[40–45]. In this content, the first-row 3d-metal cobalt-catalyzed C–H functionalization has gained increasing popularity owing to its earth-abundance, low toxicity, and distinctive reactivities[46–53], which has been largely developed for the synthesis of various skeletons by Ackermann[54–56], Yoshino and Matsunaga[57–60], Cramer[61–63], Shi[64–69], and our groups[70–73]. Very recently, our group[70], and Shi's group[65] independently developed an efficient chiral Co/Salox (salicyl-oxazoline) system, and demonstrated its excellent reactivity for assembling C–N and C–C axially chiral compounds. This strategy features significant advantages, making easily available cobalt salt catalyzed C–H functionalization for constructing axial chiral compounds being a promising research area. On the other hand, the nitrogen atoms in the N–N atropisomers may be derived from different substructures, giving rise to the possibility of forming diverse N–N axially chiral compounds. However, to the best of our knowledge, the construction of N–N axially chiral atropisomers via earth abundant transition-metal catalyzed C–H activation remains unprecedented.

Inspired by the elegant and well-established cobalt-catalyzed C–H activation/functionalization developments, and with our continuing interest in cobalt catalysis, we hope to achieve further development in this field through the strategy of direct asymmetric C–H activation. Delightedly, we here reported a highly efficient example of cobalt-catalyzed atroposelective construction of N–N axially chiral frameworks, combining the advantages of excellent efficiency and enatioselectivities (up to 98% yield and 99% e.e.) based on cobalt/Salox catalysis, which undoubtfully broaden the synthetic strategies for the direct and effective construction of N–N atropisomers and further enrich the types/scopes of N–N axially chiral derivatives. This approach has proved to be a highly suitable way for efficient preparation of N–N atropisomers according to their readily available raw materials, and accessible operation characteristics (Fig. 1c). Notable features of this protocol include: (1) the cheap cobalt(II) salt enabled N–N chiral axis construction, (2) the use of environmentally friendly O_2 as the oxidant, (3) high yields and excellent enantioselectivities with good functional group tolerance, (4) successful application under electrochemical conditions, (5) the unique atropostability for the N–N axially chiral products.

Results

Optimizing reaction conditions

To validate the feasibility of the hypothesis, our investigation was initiated by using the *N*-(7-azaindole)benzamide **1a** and phenylacetylene **2a** as the model substrates, with 10 mol% of $Co(OAc)_2{\cdot}4H_2O$ as the catalyst and O_2 as the oxidant (Table 1). Diverse chiral Salox ligands

https://doi.org/10.1038/s41467-023-40978-4

Table 1 | Optimization studies[a]

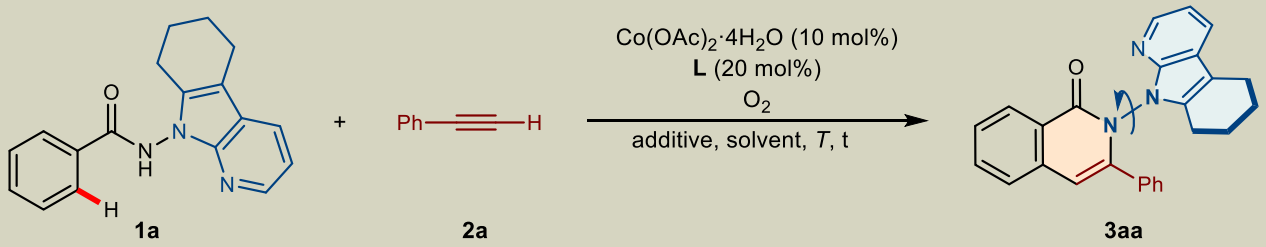

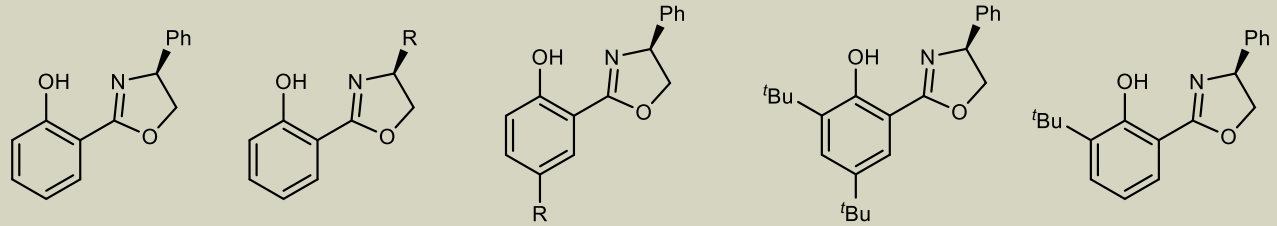

Entry	Ligand	Co catalyst	Additive	Solvent	T (°C)	Time	Yield (%)	ee (%)
1	**L6**	$Co(OAc)_2·4H_2O$	–	Toluene	100	6	48	99
2	**L6**	$Co(OAc)_2$	–	Toluene	100	6	48	98
3	**L6**	$Co(OBz)_2$	–	Toluene	100	6	45	98
4	**L6**	$CoCl_2·6H_2O$	–	Toluene	100	6	0	-
5	**L6**	$Co(OAc)_2·4H_2O$	–	1,4-Dioxane	100	6	68	98
6	**L6**	$Co(OAc)_2·4H_2O$	–	THF	100	6	42	98
7	**L6**	$Co(OAc)_2·4H_2O$	–	DME	100	6	43	98
8	**L6**	$Co(OAc)_2·4H_2O$	–	CPME	100	6	57	98
9	**L6**	$Co(OAc)_2·4H_2O$	$NaOPiv·H_2O$	1,4-Dioxane	100	6	72	98
10	**L6**	$Co(OAc)_2·4H_2O$	AcOH	1,4-Dioxane	100	6	69	98
11	**L6**	$Co(OAc)_2·4H_2O$	$AdCO_2H$	1,4-Dioxane	100	6	94	98
12	**L6**	$Co(OAc)_2·4H_2O$	$AdCO_2H$	1,4-Dioxane	80	6	94	98[b]
13	**L6**	$Co(OAc)_2·4H_2O$	$AdCO_2H$	1,4-Dioxane	80	4	89	98

ee enantiomeric excess, *N.R.* no reaction, *THF* tetrahydrofuran, *DME* 1,2-dimethoxyethane, *CPME* cyclopentyl methyl ether.

[a]Unless otherwise mentioned, all reactions were carried out using **1a** (0.1 mmol), **2a** (0.12 mmol), $Co(OAc)_2·4H_2O$ (0.01 mmol), **L6** (0.02 mmol) in toluene (1 mL) at 100 °C under O_2 for 6 h, isolated yields.

[b]90% yield and 98% ee for 0.2 mmol scale.

https://doi.org/10.1038/s41467-023-40978-4

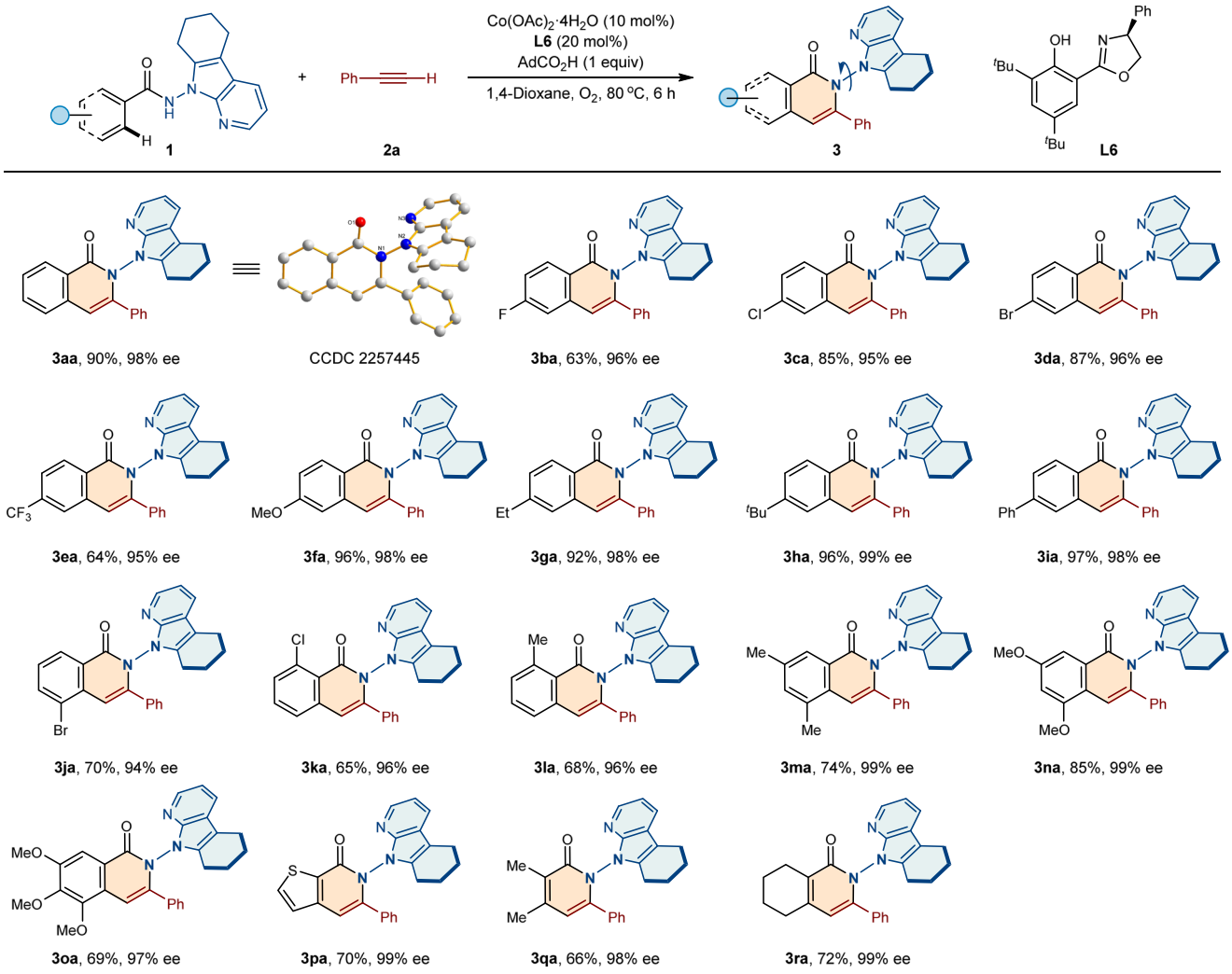

Fig. 2 | Scope of benzamides. Reaction conditions: **1** (0.2 mmol), **2a** (0.24 mmol), $Co(OAc)_2{\cdot}4H_2O$ (0.02 mmol), **L6** (0.04 mmol), $AdCO_2H$ (0.2 mmol) in 1,4-dioxane (2 mL) at 80 °C under O_2 for 6 h, isolated yields. ee, enantiomeric excess.

L1–**L7** were evaluated. It was pleased to find that the desired N–N axially chiral isoquinolinone product **3aa** was obtained with 48% yield and excellent 99% ee, with **L6** bearing bulky *tert*-butyl groups at the *ortho*- and *para*-position of phenol as the chiral ligand. And this promoting effect of the bulky ^{t}Bu-Salox ligand has also been reported in the previous Co/Salox catalysis developed by Shi[69], Ackermann[56] and our group[73]. Various cobalt catalysts, such as $Co(OAc)_2$, and $Co(OBz)_2$, $CoCl_2{\cdot}6H_2O$, were fully investigated, in which no better results have got (entries 1–4, and Supplementary Table 2). The effects of the solvent were then screened, and 1,4-dioxane displayed the best activity (entries 5–8, and Supplementary Table 3). Further optimization was conducted by the use of additives, such as $NaOPiv{\cdot}H_2O$, AcOH, and $AdCO_2H$ (entries 9–11, and Supplementary Table 4), and $AdCO_2H$ proved to be the best choice. Further optimization of the reactive temperature, time, and catalyst/ligand loadings, revealed that the reaction was able to produce the atroposelective isoquinolinone **3aa** with 94% yield and 98% ee at 80 °C for 6 h (entries 12–13, and Supplementary Tables 5–8). The absolute configuration of N–N axially chiral **3aa** was determined to be R_a by X-ray diffraction analysis (CCDC 2257445). In addition, a competitive experiment by using **1a** and **1a'** bearing a 7-methyl-8-aminoquinoline directing group with a 1:1 ratio as substrate was conducted under optimized conditions, and the product **3aa** and **3aa'** were obtained with a total yield of 99% with a 1:1 ratio (See Supplementary Table 10).

Substrate scope

With the optimal conditions in hand, we then explored the substrate generality of this transformation (Fig. 2). A variety of benzamides with diverse functionalities at *para*-position were systematically investigated. To our delight, both electron-withdrawing (−F, −Cl, −Br and $-CF_3$) and electron-donating (−OMe, −Et, −^{t}Bu, and −Ph) groups were well tolerated to afford the N–N axially chiral isoquinolinones **3ba**–**3ia** in good yields (63–97%) and excellent enantioselectivities (95 – 99% ee). For the *meta*-substituted substrate **1j**, the annulation took place at the sterically more hindered position to provide **3ja** in 70% yield and 94% ee. *Ortho*-substituted benzamides **1k** and **1l** also reacted smoothly, delivering **3ka** and **3la** with good yields and high enantiopurities of 96% ee. When multi-functionalized substrates with methyl or methoxy substituents located at the aromatic ring, the desired N–N axially chiral isoquinolinones **3ma**–**3oa** could also be obtained with good to excellent efficiencies and enantioselectivities. Notably, the heterocyclic substrate **1p** containing a thienyl moiety also reacted smoothly to give the product **3pa** with 70% yield and 99% ee. In addition, the challenging vinylamides **1q** and **1r** were well compatible with this atroposelective transformation, delivering products **3qa** and **3ra** with high level of enantiocontrol (98–99% ee).

Alkyne substrates were further expanded to verify the generality of the protocol. As shown in Fig. 3, both electron-donating (−OMe) and electron-withdrawing ($-CF_3$) groups at the *para*-position of

https://doi.org/10.1038/s41467-023-40978-4

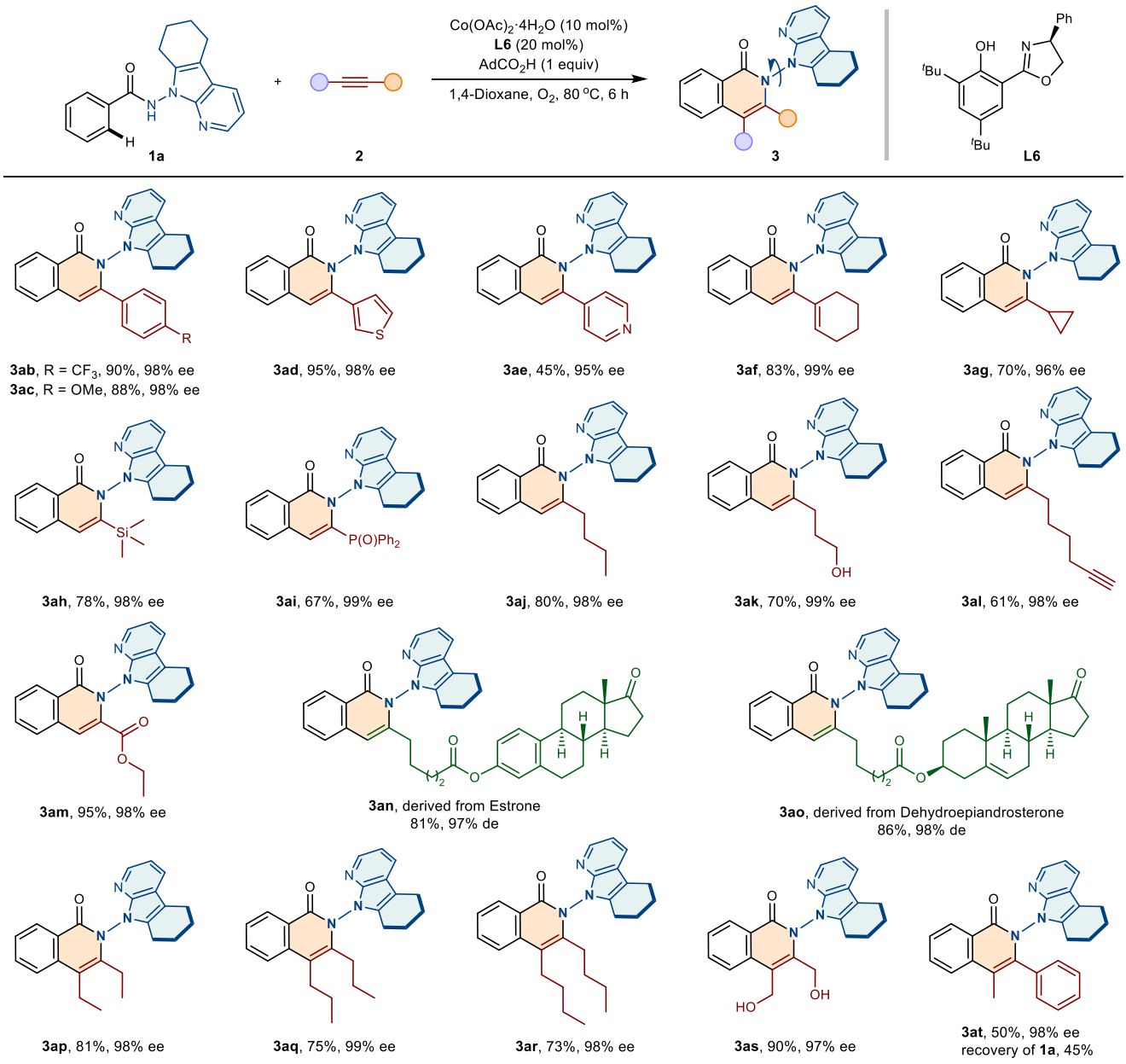

Fig. 3 | Scope of alkynes. Reaction conditions: **1a** (0.2 mmol), **2** (0.24 mmol), $Co(OAc)_2{\cdot}4H_2O$ (0.02 mmol), **L6** (0.04 mmol), $AdCO_2H$ (0.2 mmol) in 1,4-dioxane (2 mL) at 80 °C under O_2 for 6 h, isolated yields. de, diastereomeric excess.

phenylacetylene were well tolerated, and the corresponding products **3ab** and **3ac** were obtained in 90 yield, 98% ee and 88% yield, 98% ee, respectively. The heterocycle-substituted alkynes (including 3-ethynylthiophene and 4-ethynylpyridine), conjugated enyne, and cyclopropyl acetylene were also found to be compatible with this reaction, furnishing the desired products **3ad**–**3ag** with excellent enetioselectivities (95–99% ee). Notably, the presences of Si and P substituents in the resulting N–N axially chiral products (**3ah**–**3ai**) were particularly important for further derivation owing to their inherent reactivity. In addition, the alkyl or ester-substituted terminal alkynes, even with functional groups, proved to be suitable coupling partners to give products **3aj**–**3am** with good yields (61–95%) and high enantiopurities (98 – 99%). To further demonstrate the practicality of the protocol, the natural product-linked alkynes **2n** and **2o** were synthesized and utilized for the related atroposelective annulation, and the target products were successfully obtained in 81–86% yields and high diastereomeric excess (97–98% de). Moreover, the aliphatic internal alkynes **2p** – **2s** also reacted smoothly to deliver N–N axially chiral isoquinolinones **3ap**–**3as** with 97–99% ee values. For the unsymmetrical internal alkyne **2t**, the reaction proceeded with exclusive regioselectivity to give **3at** in moderate yield and high enantioselectivity, and the starting material of **1a** was recovered with a 45% yield. But the diphenylacetylene was incompatible in this system, possibly due to the steric hindrance.

Subsequently, the scope of the benzamides bearing different substituents on the 7-azaindole ring were investigated. As shown in Fig. 4, for azaindole backbone, which was functionalized by cyclohexane moiety, was well compatible, generating **3sa** in good yield (85%) and high enantiopurity (97% ee). The protocol also tolerated 2-ethyl and 2-methyl substituted azaindoles, furnishing the desired products **3ta** and **3ua** with high enantiocontrol (98% ee and 97% ee, respectively). In addition, benzamides bearing functionalities located on the C2 and C3 position of the azaindole ring, reacted smoothly to deliver N–N axially chiral products **3va**-**3xa**, with good

reactivities (70–81% yields) and excellent enantioselectivities (97–98 % ee).

To gain more efficiencies into the reactive practicality, related electrochemical experiments were conducted (Fig. 5). The general substrates were also compatible to afford the corresponding N–N axially chiral isoquinolinones **3aa** and **3ia** without any reduction of enantioselectivities. For silicon and dialkyl substituents based on alkynes, the current protocol also proved to be a powerful tactic for diverse N–N axially chiral frameworks (**3ah** and **3aq**).

Study on product stability and synthetic applications

To further explore the conformational stability of N–N axially chiral isoquinolinones, the racemization experiments were investigated (Fig. 6). Initially, the newly formed **3aa** was heated up to 160 °C in dodecane, and the ee value can be maintained without decreasing. The ee value of **3aa** decreased by 0.53% after 10 h at 180 °C. And the rotational energy barrier of **3aa** was calculated to be 41.6 kcal/mol, and its half-life ($t_{1/2}$) was up to 5.5×10^9 years at 25 °C. As the experimental results shown, energy barrier and the $t_{1/2}$ of **3aq** and **3ua** were also exhibited, indicating that the N–N axially chiral isoquinolinones endowed a high degree of atropostabilities. It is worth noting that the compounds **3aa, 3aq**, and **3ua** underwent slight decomposition after being heated for 6 or 10 h. And the recovery rates for **3aa, 3aq**, and **3ua** were 70%, 60%, and 90%, respectively. To verify the accuracy of the testing rotational energy barriers, we further studied the enantiomerization processes of **3aa** and **3ua** by DFT calculations. As shown in Fig. 6 and Supplementary Fig. 6, the energy barriers of the dihedral rotation via transition states $\mathbf{TS}^{3aa}$ and $\mathbf{TS}^{3ua}$ are 40.3 kcal/mol and 41.2 kcal/mol respectively, which showed good agreement with the experimental results.

The gram-scale experiment using **1a** (3.5 mmol, 1.02 g) with **2a** under standard conditions delivered **3aa** without obvious decrease in yield and enantioselectivity (88% yield, 96% ee). Furthermore, the annulation of **1a** with diphenylphosphinoacetylene (**2i**) on a gram-scale was caried out, leading to the formation of phosphoryl product **3ai** with 60% yield and 99% ee (Fig. 7a). The synthetic utility of this developed protocol to access N–N atropisomers was also further highlighted by post-functionalization. The compound **3ai** was reduced to produce monophosphine product **4** with a remarkable 99% ee. In

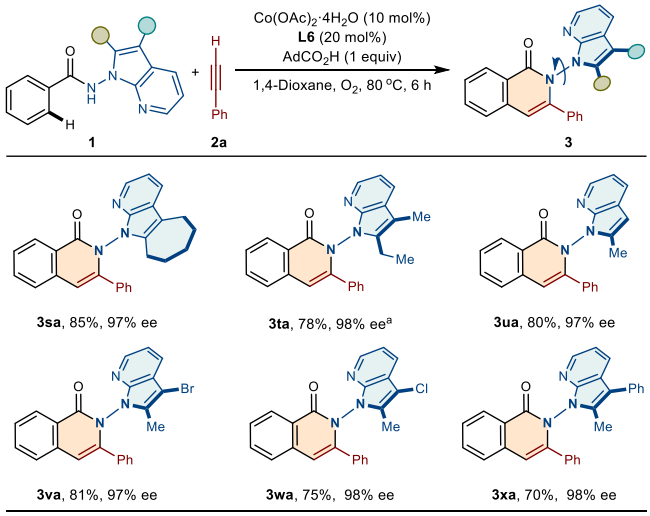

Fig. 4 | Scope of Benzamides with Substituents on the 7-Azaindole Ring. Reaction conditions: **1** (0.2 mmol), **2a** (0.24 mmol), $Co(OAc)_2{\cdot}4H_2O$ (0.02 mmol), **L6** (0.04 mmol), $AdCO_2H$ (0.2 mmol) in 1,4-dioxane (2 mL) at 80 °C under O_2 for 6 h, isolated yields. [a]20 mol% $Co(OAc)_2{\cdot}4H_2O$, 10 h. ee enantiomeric excess.

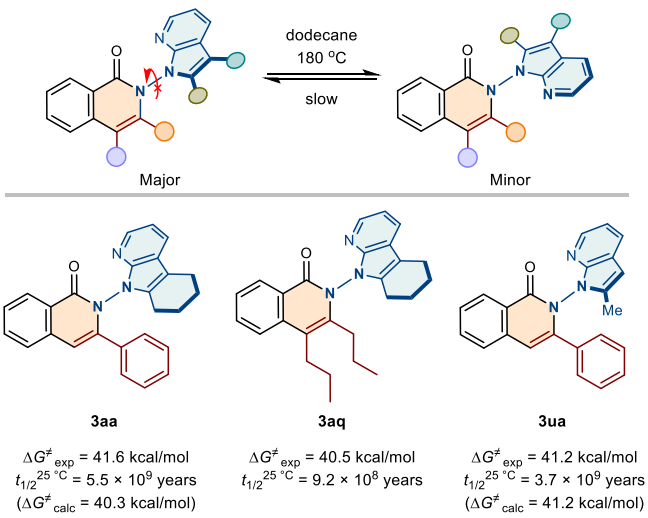

Fig. 6 | Study on product stability. The rotation barrier and the $t_{1/2}$ of **3aa, 3aq**, and **3ua**.

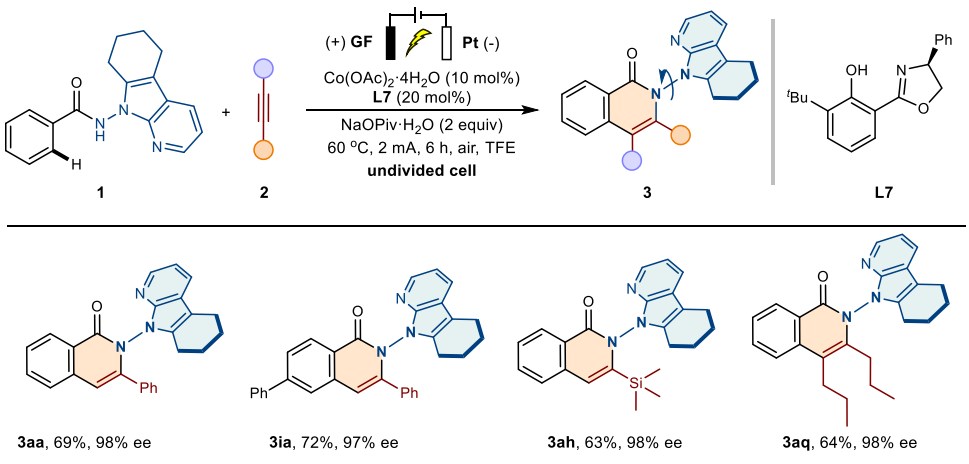

Fig. 5 | Reaction scope for the electro-oxidative annulation. Reaction conditions: graphite felt anode, Pt-plate cathode, constant current = 2 mA, **1** (0.2 mmol), **2** (0.24 mmol), $Co(OAc)_2{\cdot}4H_2O$ (0.02 mmol), **L7** (0.04 mmol), TFE (5 mL), $NaOPiv{\cdot}H_2O$ (0.4 mmol), 60 °C, 6 h, air, isolated yields. ee, enantiomeric excess; TFE, 2,2,2-trifluoroethanol.

https://doi.org/10.1038/s41467-023-40978-4

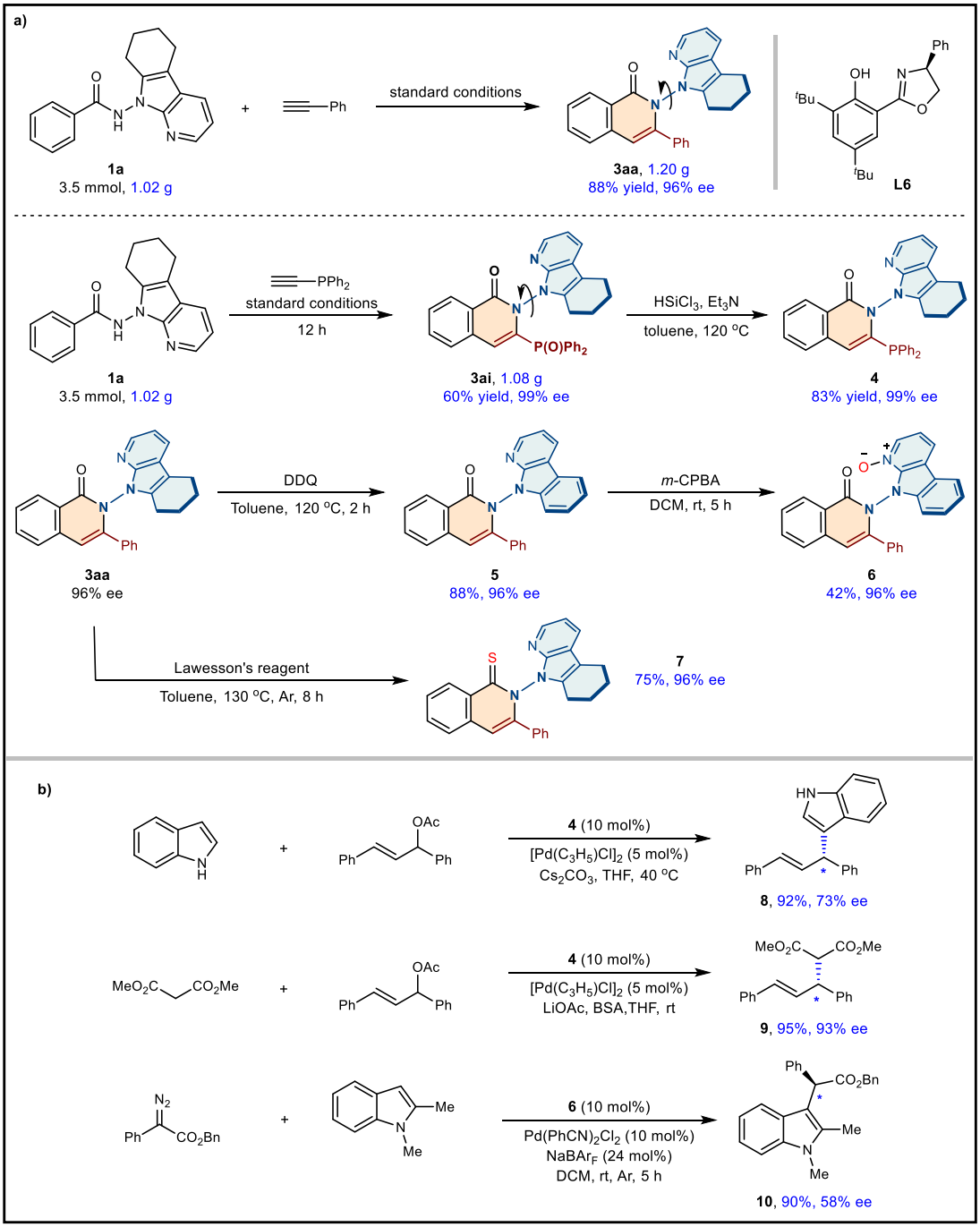

Fig. 7 | Gram-scale experiments and synthetic applications. a Gram-scale experiments using **1a** as substrates and post-functionalization of N–N axially chiral product **3aa** and **3ai**. ee, enantiomeric excess; DDQ, 2,3-dichloro-5,6-dicyano-1,4-benzoquinone; *m*-CPBA, 3-chloroperoxybenzoic acid; BSA, *N*,*O*-bis(trimethylsilyl)-acetamide; DCM, dichloromethane; THF, tetrahydrofuran; rt, roomtemperature. **b** Applications of N–N axially chiral compound **4** and **6** as chiral ligands for further applications.

addition, the oxidative product **5** could be obtained by treatment of N-N axially chiral isoquinolinone **3aa** with DDQ in 88% yield at 120 °C for 2 h. Further treatment of **5** with *m*-CPBA afforded *N*-oxide **6**. As the experimental result shown, the carbonyl group of N–N axially chiral isoquinolinone could also be easily transformed into a thiocarbonyl group in 75% yield without compromising enantioselectivity at the presence of Lawesson's reagent (Fig. 7a). Monophosphine product **4** could serve as a suitable chiral ligand for the asymmetric Pd-catalyzed allylic substitution reaction of indole and the Tsuji-Trost reaction, and the desired products were obtained with excellent yields and good to high enantioselectivities (73% ee for **8**, 93% ee for **9**). In addition, *N*-oxide **6** was regarded as the chiral ligand to react with benzyl 2-diazo-2-phenylacetate and 1,2-dimethyl-1*H*-indole in the presence of palladium catalyst to give desired **10** in 90% yield and 58% ee value (Fig. 7b)[70].

To investigate the reaction mechanism, deuterium labeling experiments were conducted. H/D exchange experiments illustrated that the C-H cleavage was irreversible (Fig. 8a). Then, the parallel and competitive kinetic isotope effect (KIE) values of 1.7 and 1.9 were calculated, indicating that C-H cleavage may be involved in the rate-determining step (Fig. 8b). Furthermore, the study on the nonlinear effect between the enantiomeric excess (ee) of product **3aa** and the ee of **L6** revealed that a single chiral ligand coordinated with a cobalt

https://doi.org/10.1038/s41467-023-40978-4

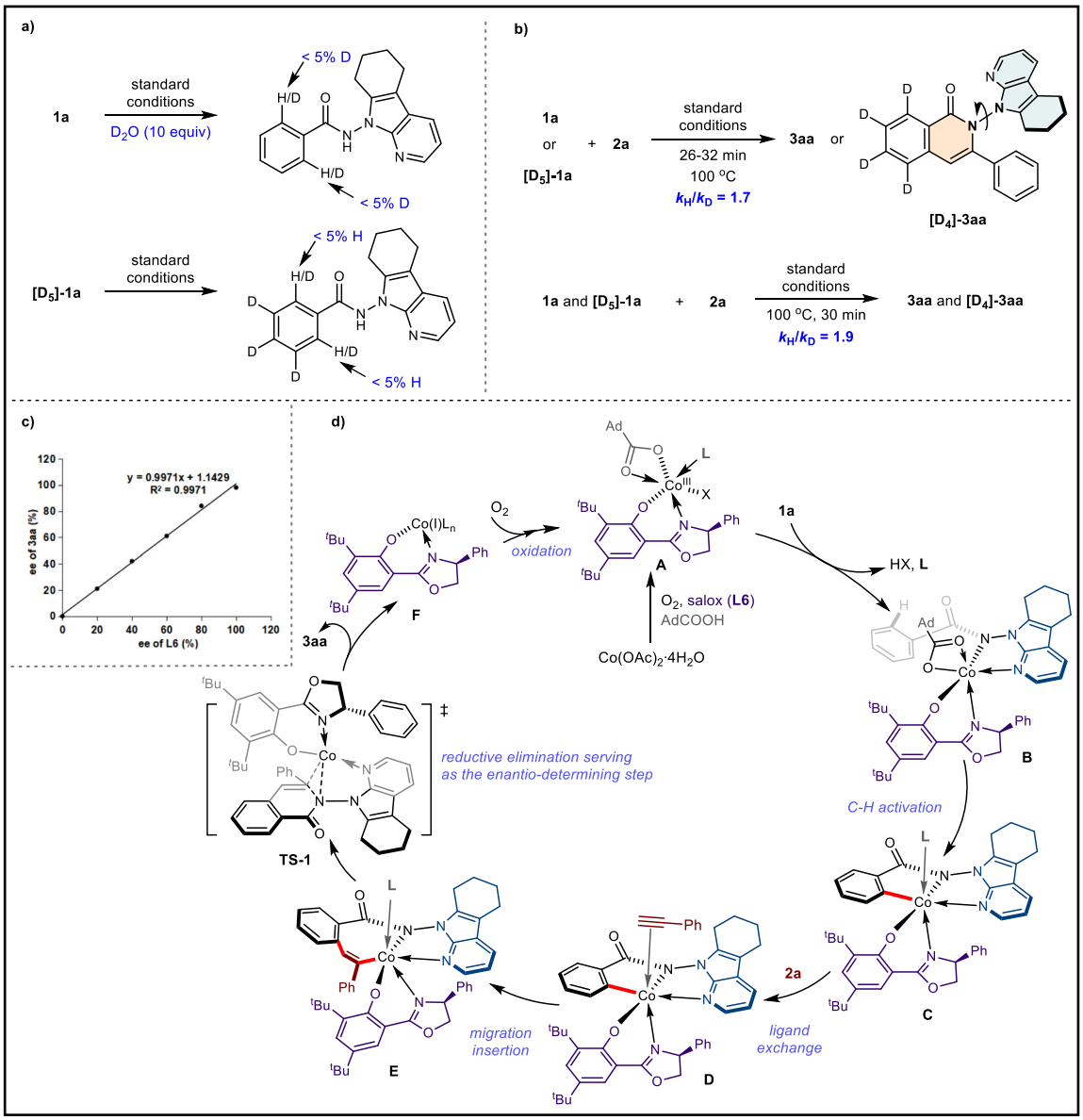

Fig. 8 | Mechanistic studies. a H/D Exchange experiments using **1a** or **[D_5]−1a** as substrates. **b** Parallel and competitive kinetic isotope experiments to calculate KIE values. **c** Nolinear effect study between the enantiomeric excess (ee) of product **3aa** and the ee of **L6**. **d** Plausible mechanism for the Co/Salox catalyzed annulation.

atom to create an effective catalyst (Fig. 8c). Based on the previous reports[65–73] and the above results, a plausible mechanism was proposed (Fig. 8d). Cobalt salt (II) coordinates with **L6** and $AdCO_2H$, and undergoes oxidation with O_2 to produce active Co(III)-species **A**, which then undergoes ligand exchange with substrate **1a** to form the octahedral Co(III)-intermediate **B**. The C−H activation of **B** affords the key intermediate **C**. It is worth mentioning that another pathway involving the first C-H activation step and the following oxidation step to form the intermediate **C** could not be completely ruled out. Next, alkyne **2a** coordinates with **C** and the ligand exchange occurred to form **D**. The migration insertion of alkyne into the C-Co bond affords the seven-membered alkenyl intermediate **E**. Finally, the reductive elimination of **E** leads to the formation of the N−N axially chiral product **3aa** and meanwhile releases the Co(I) intermediate **F**. Based on our previous report for the synthesis of C−N axially chiral compounds[70], the reductive elimination through transition states **TS-1**, which features the lowest-energy owing to the π-π stacking interactions between phenyl group of **L6** with the 7-azaindole directing group of **1a**, might serve as the enantio-determining step.

In conclusion, we have developed an efficient and facile synthetic method for accessing N−N axially chiral isoquinolinones through cobalt-catalyzed atroposelective C−H activation/annulation. This protocol exhibits several unique characteristics, including a broad substrate scope, environmentally friendly O_2 as the oxidant, and excellent efficiencies and enantioselectivities. The obtained N−N axially chiral isoquinolinones features unique atropostability, which further expands the repertoire of N−N axially chiral derivatives. In addition, this method has proven to be a powerful strategy for constructing the N−N axial architectures under electrochemical conditions for asymmetric cobalt/Salox catalysis. Furthermore, other types of N−N axially chiral compounds, and related applications to asymmetric catalysis, functional materials are being evaluated in our laboratory and will be reported in due course.

Methods

General procedure for the synthesis of compounds 3

An oven dried schleck tube charged with magnetic stirrer added benzamide/vinylamide **1** (0.2 mmol), $Co(OAc)_2{\cdot}4H_2O$ (0.02 mmol,

10 mol%), **L6** (0.04 mmol, 20 mol%), 1-adamantanecarboxylic acid (0.2 mmol, 1.0 equiv) with subsequent addition of 1,4-dioxane (2 mL) as solvent. To this reaction mixture, **2** (0.24 mmol, 1.2 eq) was added under O_2. Then, the reaction system was stirred at 80 °C for 6 h. After the reaction was completed, the reaction mixture was quenched with saturated $NaHCO_3$ solution and extracted with CH_2Cl_2. The combined organic layer extracts were washed with brine, dried over Na_2SO_4, and concentrated under reduced pressure, and purified on silica gel chromatography (petroleum ether/ethyl acetate = 5:1) to afford the corresponding products. Full experimental details and characterization of the compounds are given in the Supplementary Information.

Data availability

The X-ray crystallographic coordinates for structures reported in this study have been deposited at the Cambridge Crystallographic Data Centre (CCDC), under deposition number 2257445 (for **3aa**). These data can be obtained free of charge from The Cambridge Crystallographic Data Centre via www.ccdc.cam.ac.uk/data_request/cif. The authors declare that the data supporting the findings of this study are available within the article and its Supplementary Information Files. Cartesian coordinates of the calculated structures are available in Supplementary Data 1. All other data are available from the corresponding authors upon request.

References

1. Clayden, J., Moran, W. J., Edwards, P. J. & Laplante, S. R. The challenge of atropisomerism in drug discovery. *Angew. Chem., Int. Ed.* **48**, 6398–6401 (2009).
2. Bringmann, G., Gulder, T., Gulder, T. A. M. & Breuning, M. Atroposelective total synthesis of axially chiral biaryl natural products. *Chem. Rev.* **111**, 563–639 (2011).
3. Toenjes, S. T. & Gustafson, J. L. Atropisomerism in medicinal chemistry: challenges and opportunities. *Future Med. Chem.* **10**, 409–422 (2018).
4. Basilaia, M., Chen, M. H., Secka, J. & Gustafson, J. L. Atropisomerism in the pharmaceutically relevant realm. *Acc. Chem. Res.* **55**, 2904–2919 (2022).
5. Christie, G. H. & Kenner, J. The molecular configurations of polynuclear aromatic compounds. Part I. The resolution of g-6: 60-dinitro- and 4: 6: 40: 60-tetranitrodiphenic acids into optically active components. *J. Chem. Soc. Trans.* **121**, 614–620 (1922).
6. Perreault, S., Chandrasekhar, J. & Patel, L. Atropisomerism in drug discovery: a medicinal chemistry perspective inspired by atropisomeric class I PI3K inhibitors. *Acc. Chem. Res.* **55**, 2581–2593 (2022).
7. Wencel-Delord, J., Panossian, A., Leroux, F. R. & Colobert, F. Recent advances and new concepts for the synthesis of axially stereoenriched biaryls. *Chem. Soc. Rev.* **44**, 3418–3430 (2015).
8. Metrano, A. J. & Miller, S. J. Peptide-based catalysts reach the outer sphere through remote desymmetrization and atroposelectivity. *Acc. Chem. Res.* **52**, 199–215 (2019).
9. Zhang, Y.-C., Jiang, F. & Shi, F. Organocatalytic asymmetric synthesis of indole-based chiral heterocycles: strategies, reactions, and outreach. *Acc. Chem. Res.* **53**, 425–446 (2020).
10. Cheng, J. K. et al. Recent advances in catalytic asymmetric construction of atropisomers. *Chem. Rev.* **121**, 4805–4902 (2021).
11. Zhang, X., Zhao, K. & Gu, Z. Transition metal-catalyzed biaryl atropisomer synthesis via a torsional strain promoted ring-opening reaction. *Acc. Chem. Res.* **55**, 1620–1633 (2022).
12. Kumarasamy, E., Raghunathan, R., Sibi, M. P. & Sivaguru, J. Nonbiaryl and heterobiaryl atropisomers: molecular templates with promise for atropselective chemical transformations. *Chem. Rev.* **115**, 11239–11300 (2015).
13. Li, T.-Z., Liu, S.-J., Tan, W. & Shi, F. Catalytic asymmetric construction of axially chiral indole-based frameworks: an emerging area. *Chem. Eur. J.* **26**, 15779–15792 (2020).
14. Kitagawa, O. Chiral Pd-catalyzed enantioselective syntheses of various N–C axially chiral compounds and their synthetic applications. *Acc. Chem. Res.* **54**, 719–730 (2021).
15. Colobert, F. & Shi, B.-F. C–N atropopure compounds: new directions. *Chem. Catal.* **1**, 483–485 (2021).
16. Zhang, H.-H. & Shi, F. Organocatalytic atroposelective synthesis of indole derivatives bearing axial chirality: strategies and applications. *Acc. Chem. Res.* **55**, 2562–2580 (2022).
17. Mei, G.-J., Koay, W. L., Guan, C.-Y. & Lu, Y. Atropisomers beyond the C–C axial chirality: advances in catalytic asymmetric synthesis. *Chem* **8**, 1–39 (2022).
18. Rodríguez-Salamanca, P., Fernández, R., Hornillos, V. & Lassaletta, J. M. Asymmetric synthesis of axially chiral C-N atropisomers. *Chem. Eur. J.* **28**, e202104442 (2022).
19. Lu, C.-J., Xu, Q., Feng, J. & Liu, R.-R. The asymmetric buchwald-hartwig amination reaction. *Angew. Chem. Int. Ed.* **62**, e202216863 (2023).
20. Benincori, T. et al. Chiral atropisomeric five-membered biheteroaromatic diphosphines: new ligands of the bibenzimidazole and biindole series. *J. Organomet. Chem.* **529**, 445–453 (1997).
21. Antognazza, P. et al. Resolution and characterization of 2,2′-bis(diphenylphosphino)–1,1′-bibenzimidazole (BIMIP): the first chiral atropisomeric diphosphine ligand with hindered rotation around a N – N bon. *Phosphorus, Sulfur, Silicon Relat. Elem.* **144**, 405–408 (1999).
22. Zhang, Q. et al. N–N-coupled indolo-sesquiterpene atropo-diastereomers from a marine-derived actinomycete. *Eur. J. Org. Chem.* **2012**, 5256–5262 (2012).
23. Xu, Z., Baunach, M., Ding, L. & Hertweck, C. Bacterial synthesis of diverse indole terpene alkaloids by an unparalleled cyclization sequence. *Angew. Chem. Int. Ed.* **51**, 10293–10297 (2012).
24. Blair, L. M. & Sperry, J. Natural products containing a nitrogen–nitrogen bond. *J. Nat. Prod.* **76**, 794–812 (2013).
25. Kobayashi, T. et al. Analysis of interconversion between atropisomers of chiral substituted 9,9′-bicarbazole. *Eur. J. Org. Chem.* **2021**, 449–451 (2021).
26. Verma, S. M. & Prasad, R. Conformational analysis by nuclear magnetic resonance spectroscopy. N′-derivatives of N-aminocamphorimides. *J. Org. Chem.* **38**, 1004–1010 (1973).
27. Mei, G.-J. et al. Rational design and atroposelective synthesis of N–N axially chiral compounds. *Chem* **7**, 2743–2757 (2021).
28. Lin, W. et al. Asymmetric synthesis of N–N axially chiral compounds *via* organocatalytic atroposelective N-acylation. *Chem. Sci.* **13**, 141–148 (2022).
29. Pan, M., Shao, Y.-B., Zhao, Q. & Li, X. Asymmetric synthesis of N–N axially chiral compounds by phase-transfer-catalyzed alkylations. *Org. Lett.* **24**, 374–378 (2022).
30. Portolani, C. et al. Synthesis of atropisomeric hydrazides by one-pot sequential enantio- and diastereoselective catalysis. *Angew. Chem. Int. Ed.* **61**, e202209895 (2022).
31. Wang, X.-M. et al. Enantioselective synthesis of nitrogen–nitrogen biaryl atropisomers via copper-catalyzed friedel-crafts alkylation reaction. *J. Am. Chem. Soc.* **143**, 15005–15010 (2021).
32. Xu, Q. et al. Cu(I)-catalyzed asymmetric arylation of pyrroles with diaryliodonium salts toward the synthesis of N–N atropisomers. *Org. Lett.* **24**, 3138–3143 (2022).
33. Pu, L.-Y., Zhang, Y.-J., Liu, W. & Teng, F. Chiral phosphoric acid-catalyzed dual-ring formation for enantioselective construction of N–N axially chiral 3,3′-bisquinazolinones. *Chem. Commun.* **58**, 13131–13134 (2022).
34. Gao, Y. et al. Atroposelective synthesis of 1,1′-bipyrroles bearing a chiral N – N axis: chiral phosphoric acid catalysis with lewis acid

induced enantiodivergence. *Angew. Chem. Int. Ed.* **61**, e202200371 (2022).
35. Zhang, P. et al. Enantioselective synthesis of N – N bisindole atropisomers. *Angew. Chem. Int. Ed.* **61**, e202212101 (2022).
36. Chen, K.-W. et al. Organocatalytic atroposelective synthesis of N – N axially chiral indoles and pyrroles by de novo ring formation. *Angew. Chem. Int. Ed.* **61**, e202116829 (2022).
37. Chen, Z.-H. et al. Organocatalytic enantioselective synthesis of axially chiral N,N′-bisindoles. *Angew. Chem. Int. Ed.* **62**, e202300419 (2023).
38. Yin, S.-Y., Zhou, Q., Liu, C.-X., Gu, Q. & You, S.-L. Enantioselective synthesis of N–N biaryl atropisomers through iridium(I)-catalyzed C-H alkylation with acrylates. *Angew. Chem. Int. Ed.* **62**, e202305067 (2023).
39. Yao, W. et al. Enantioselective synthesis of N – N atropisomers by palladium-catalyzed C-H functionalization of pyrroles. *Angew. Chem. Int. Ed.* **62**, e202218871 (2023).
40. Wencel-Delord, J. & Glorius, F. C-H bond activation enables the rapid construction and late-stage diversification of functional molecules. *Nat. Chem.* **5**, 369–375 (2013).
41. Newton, C. G., Wang, S.-G., Oliveira, C. C. & Cramer, N. Catalytic enantioselective transformations involving C-H bond cleavage by transition-metal complexes. *Chem. Rev.* **117**, 8908–8976 (2017).
42. Saint-Denis, T. G. et al. Enantioselective C(sp^3)–H bond activation by chiral transition metal catalysts. *Science* **359**, eaao4798 (2018).
43. Abrams, D. J., Provencher, P. A. & Sorensen, E. J. Recent applications of C-H functionalization in complex natural product synthesis. *Chem. Soc. Rev.* **47**, 8925–8967 (2018).
44. Achar, T. K., Maiti, S., Jana, S. & Maiti, D. Transition metal catalyzed enantioselective C(sp^2)–H bond functionalization. *ACS Catal.* **10**, 13748–13793 (2020).
45. Zhang, Q., Wu, L.-S. & Shi, B.-F. Forging C-heteroatom bonds by transition-metal-catalyzed enantioselective C-H functionalization. *Chem* **8**, 384–413 (2022).
46. Moselage, M., Li, J. & Ackermann, L. Cobalt-catalyzed C-H activation. *ACS Catal.* **6**, 498–525 (2015).
47. Kommagalla, Y. & Chatani, N. Cobalt(II)-catalyzed C-H functionalization using an N,N′-bidentate directing group. *Coord. Chem. Rev.* **350**, 117–135 (2017).
48. Woźniak, Ł. & Cramer, N. Enantioselective C-H bond functionalizations by 3d transitionmetal catalysts. *Trends Chem.* **1**, 471–484 (2019).
49. Loup, J. et al. Enantioselective C – H activation with earth-abundant 3d transition metals. *Angew. Chem. Int. Ed.* **58**, 12803–12818 (2019).
50. Gandeepan, P. et al. 3d Transition metals for C-H activation. *Chem. Rev.* **119**, 2192–2452 (2019).
51. Yoshino, T. & Matsunaga, S. Chiral carboxylic acid assisted enantioselective C-H activation with achiral Cp^xM^{III} (M = Co, Rh, Ir) catalysts. *ACS Catal.* **11**, 6455–6466 (2021).
52. Mandal, R., Garai, B. & Sundararaju, B. Weak-coordination in C-H bond functionalizations catalyzed by 3d metals. *ACS Catal.* **12**, 3452–3506 (2022).
53. Zheng, Y., Zheng, C., Gu, Q. & You, S.-L. Enantioselective C-H functionalization reactions enabled by cobalt catalysis. *Chem. Catal.* **2**, 2965–2985 (2022).
54. Zell, D. et al. Full selectivity control in cobalt(III)- catalyzed C – H alkylations by switching of the C – H activation mechanism. *Angew. Chem. Int. Ed.* **56**, 10378–10382 (2017).
55. Pesciaioli, F. et al. Enantioselective cobalt(III)-catalyzed C – H activation enabled by chiral carboxylic acid cooperation. *Angew. Chem., Int. Ed.* **57**, 15425–15429 (2018).
56. Münchow, T. V. et al. Enantioselective electrochemical cobalt-catalyzed aryl C–H activation reactions. *Science* **379**, 1036–1042 (2023).
57. Sekine, D. et al. Chiral 2-aryl ferrocene carboxylic acids for the catalytic asymmetric C(sp^3)–H activation of thioamides. *Organometallics* **38**, 3921–3926 (2019).
58. Fukagawa, S. et al. Enantioselective C(sp 3)- H amidation of thioamides catalyzed by a cobalt III /chiral carboxylic acid hybrid system. *Angew. Chem. Int. Ed.* **58**, 1153–1157 (2019).
59. Kurihara, T., Kojima, M., Yoshino, T. & Matsunaga, S. Cp^*Co^{III}/chiral carboxylic acid-catalyzed enantioselective 1,4-addition reactions of indoles to maleimides. *Asian J. Org. Chem.* **9**, 368–371 (2020).
60. Hirata, Y. et al. Cobalt(III)/chiral carboxylic acid-catalyzed enantioselective synthesis of benzothiadiazine-1-oxides via C-H activation. *Angew. Chem. Int. Ed.* **61**, e202205341 (2022).
61. Ozols, K., Jang, Y.-S. & Cramer, N. Chiral cyclopentadienyl cobalt(III) complexes enable highly enantioselective 3d-metalcatalyzed C-H functionalizations. *J. Am. Chem. Soc.* **141**, 5675–5680 (2019).
62. Ozols, K., Onodera, S., Woźniak, Ł. & Cramer, N. Cobalt(III)-catalyzed enantioselective intermolecular carboamination by C – H functionalization. *Angew Chem. Int. Ed.* **60**, 655–659 (2021).
63. Herraiz, A. G. & Cramer, N. Cobalt(III)-catalyzed diastereo- and enantioselective three-component C-H functionalization. *ACS Catal.* **11**, 11938–11944 (2021).
64. Zhou, Y.-B. et al. Synthesis of sulfur-stereogenic sulfoximines via Co(III)/chiral carboxylic acid-catalyzed enantioselective C-H amidation. *ACS Catal.* **12**, 9806–9811 (2022).
65. Wang, B.-J. et al. Single-step synthesis of atropisomers with vicinal C-C and C-N diaxes by cobalt-catalyzed atroposelective C-H annulation. *Angew. Chem. Int. Ed.* **61**, e202208912 (2022).
66. Yao, Q.-J. et al. Cobalt/salox-catalyzed enantioselective C-H functionalization of arylphosphinamides. *Angew Chem. Int. Ed.* **61**, e202202892 (2022).
67. Chen, J.-H. et al. Cobalt/salox-catalyzed enantioselective dehydrogenative C-H alkoxylation and amination. *Angew. Chem. Int. Ed.* **61**, e202210106 (2022).
68. Zhou, G. et al. Base-promoted electrochemical Co(II)-catalyzed enantioselective C – H oxygenation. *Angew. Chem. Int. Ed.* **62**, e202302964 (2023).
69. Yao, Q.-J., Huang, F.-R., Chen, J.-H., Zhong, M.-Y. & Shi, B.-F. Enantio- and regioselective electrooxidative cobalt-catalyzed C-H/N-H annulation with alkenes. *Angew. Chem. Int. Ed.* **62**, e202218533 (2023).
70. Si, X.-J. et al. Atroposelective isoquinolinone synthesis through cobalt-catalysed C-H activation and annulation. *Nat. Synth.* **1**, 709–718 (2022).
71. Professional comments on ref 15a: Kikuchi, J. & Yoshikai, N. Cobalt selectively annulates. *Nat. Synth.* **1**, 674–675 (2022).
72. Yang, D. et al. Cobalt-catalyzed enantioselective C–H annulation with alkenes. *ACS Catal.* **13**, 4250–4260 (2023).
73. Si, X.-J. et al. Cobalt-catalyzed enantioselective C–H/N–H annulation of aryl sulfonamides with allenes or alkynes: facile access to C–N axially chiral sultams. *Chem. Sci.* **14**, 7291–7303 (2023).

Acknowledgements

We thank for the support of the National Natural Science Foundation of China (22271260 to J.-L.N.; 22101267 to L.S.), and Natural Science Foundation of Henan Province (222300420291 to D.Y.).

Author contributions

J.-L.N., D.Y., and L.S. conceived the concept and prepared the manuscript. T.L., X.W., and C.Y. conducted the experiments and analyzed the data. M.-P.S. provided revisions. All the authors participated in the

discussion and preparation of the manuscript. J.-L.N., D.Y., and L.S. directed the project.

Competing interests
The authors declare no competing interests.

Additional information
Supplementary information The online version contains supplementary material available at https://doi.org/10.1038/s41467-023-40978-4.

Correspondence and requests for materials should be addressed to Dandan Yang or Jun-Long Niu.

Peer review information *Nature Communications* thanks Naohiko Yoshikai and the other, anonymous, reviewer(s) for their contribution to the peer review of this work. A peer review file is available.